Eur. Phys. J. C (2018) 78:210
https://doi.org/10.1140/epjc/s10052-018-5702-7

THE EUROPEAN PHYSICAL JOURNAL C

Regular Article - Theoretical Physics

Disclosing $D^*\bar{D}^*$ molecular states in the $B_c^- \to \pi^- J/\psi\omega$ decay

L. R. Dai[1,2,a], **J. M. Dias**[2,3,b], **E. Oset**[2,c]

[1] Department of Physics, Liaoning Normal University, Dalian 116029, China
[2] Departamento de Física Teórica and IFIC, Institutos de Investigación de Paterna, Centro Mixto Universidad de Valencia-CSIC, Apartado 22085, 46071 Valencia, Spain
[3] Instituto de Física, Universidade de São Paulo, Rua do Matão, 1371 Butantã, São Paulo, São Paulo CEP 05508-090, Brazil

Received: 25 January 2018 / Accepted: 3 March 2018 / Published online: 13 March 2018

Abstract We study the $B_c^- \to \pi^- J/\psi\omega$ and $B_c^- \to \pi^- D^*\bar{D}^*$ reactions and show that they are related by the presence of two resonances, the $X(3940)$ and $X(3930)$, that are of molecular nature and couple most strongly to $D^*\bar{D}^*$, but also to $J/\psi\omega$. Because of that, in the $J/\psi\omega$ mass distribution we find a cusp with large strength at the $D^*\bar{D}^*$ threshold and predict the ratio of strengths between the peak of the cusp and the maximum of the $D^*\bar{D}^*$ distribution close to $D^*\bar{D}^*$ threshold, which are distinct features of the molecular nature of these two resonances.

1 Introduction

Molecular states of mesons have long been the subject of study in hadron physics. Detailed recent reviews can be seen in Refs. [1,2]. As commented in Ref. [3] the support for hadron molecules is quite obvious once we realize that baryon molecules exist in the form of nuclei. In fact, multi-mesons states, not just meson-meson molecules, have also been advocated, like multi-rho states in Ref. [4], K^*-multi-rho states in Ref. [5], D^*-multi-rho states in Ref. [6], two mesons and a baryon states [7,8] and many others (see a recent review in Ref. [9]). Actually, the interaction between mesons, particularly vector mesons in spin two, is very strong [10–12], even stronger than between nucleons, and the only limit to the formation of multi-meson states is that we do not have the meson number conservation, unlike baryon number conservation for the nucleons forming nuclei. This allows the multi-meson states to decay in states of fewer, or lighter mesons, the width increases with the number of mesons of the cluster, and at some point they are no longer identifiable experimentally. Even then, according to [4–6], states up to 6 vector mesons can be detected and the $f_6(2510)$ qualifies as a six-rho meson state [4].

The identification of states as being of molecular nature is not an easy task, and in general standard quark structures, or multiquark states are competing in the interpretation [1,3]. Yet, there are several experimental features that reveal the molecular structure [2] and ultimately it is the systematic and correct description of experimental features and the accuracy of the predictions what builds up in favor of this structure for many states.

The weak decay of heavy mesons and baryons has turned out into one important tool to identify states of molecular type [13]. Curiously, an interaction that does not respect parity and isospin, has shown itself as a great tool to identify molecular states because certain decays filter good quantum numbers due to selection rules, like Cabibbo and color enhancement in some topologies of decay modes.

One of the features attached to the molecular states that couple to several hadron-hadron channels, is that by looking at one of the channels with relatively small strength one finds a strong and unexpected cusp in the threshold of the channels corresponding to the main component of the molecule. One recent example of this was found in the $B^+ \to J/\psi\phi K^+$ reaction measured at LHCb [14,15]. The reaction was analyzed in [14,15] and at low invariant masses only the $X(4140)$ state was included, concluding that its width had to be considerably larger than the average of the PDG [16] from other experiments. A different interpretation, with a better fit to the data, was given in [17], where, in addition to the $X(4140)$, the $X(4160)$ was included in the fit, assuming that this state is the $D_s^*\bar{D}_s^*$ state predicted in [18] as a $I^G[J^{PC}] = 0^+[2^{++}]$ state. It is worth noting that other works have also suggested a bound state of $D_s^*\bar{D}_s^*$ [19–22], although it was originally associated to the $X(4140)$. This bound $D_s^*\bar{D}_s^*$ state also couples to other light vector states and to $J/\psi\phi$, hence, it can be observed in this latter channel. However, the fact that the

[a] e-mail: dailr@lnnu.edu.cn
[b] e-mail: jdias@if.usp.br
[c] e-mail: oset@ific.uv.es

resonance couples most strongly to $D_s^* \bar{D}_s^*$ has the consequence that the $J/\psi\phi$ mass spectrum develops a strong cusp at the $D_s^* \bar{D}_s^*$ threshold, something visible in the experimental spectra with an increased strength in that region. It is also worth mentioning that a similar enhancement is seen, although with poor statistics, in the recent BESIII work on the $e^+e^- \to \gamma J/\psi\phi$ reaction [23].

In the present work we want to continue along this line of research and present results for a reaction that should reveal the $D^*\bar{D}^*$ nature of two states found in [18] as $0^+[0^{++}]$ and $0^+[2^{++}]$ at 3943 and 3922 MeV, respectively, which can be identified with some experimental states in that region [16,18].[1]

In this case we note that the states found, mostly $D^*\bar{D}^*$ bound states, also couple to $J/\psi\omega$ in the second place, and $J/\psi\phi$ with smaller strength. So we choose the $J/\psi\omega$ observation channel looking into the necessary cusp that should develop at the $D^*\bar{D}^*$ threshold. For this purpose we look into the $B_c^- \to \pi^- J/\psi\omega$ decay and then into the $J/\psi\omega$ invariant mass distribution. The choice of this reaction is that in a first stage of the reaction the $D^*\bar{D}^*$ state is formed with a dominant weak decay mechanism, but the $J/\psi\omega$ state is not formed at this level. Then the $J/\psi\omega$ is finally produced via rescattering of the $D^*\bar{D}^*$ component with the other components that make up the two molecular states. This stresses the role of the resonance since there is no tree level $J/\psi\omega$ contribution. Thus, we obtain two peaks in the $J/\psi\omega$ mass distribution corresponding to the molecular states and a strong cusp at the $D^*\bar{D}^*$ threshold. In addition we also look at the $D^*\bar{D}^*$ mass distribution in the $B_c^- \to \pi^- D^*\bar{D}^*$ reaction and evaluate its strength above the $D^*\bar{D}^*$ threshold, which is closely connected to the strength of the $J/\psi\omega$ mass distribution. The $D^*\bar{D}^*$ cusp feature, together with the relative strength of the $D^*\bar{D}^*$ compared to the one of $J/\psi\omega$, are two magnitudes which are tied to the molecular structure of these two resonances, and we encourage the performance of the experiment that should bring valuable light into these issues.

[1] The state at 3943 MeV can be associated with the $X(3940)$ of [24,25] and the $X(3922)$ with the $X(3930)$[27] now classified in the PDG as the $\chi_{c2}(2P)$. The width of the $X(3943)$ MeV obtained in [18] of 15–17 MeV looks small compared to $\Gamma = 87 \pm 22 \pm 26$ MeV of [24]. These results are improved in [25] by measuring the $D\bar{D}$ and $D\bar{D}^*$ decay channels with $\Gamma = 15.4 \pm 10.1$ MeV, in good agreement with the results of [18]. A further experiment for the $X(3940)$ in [26] from the measurement of the $D^*\bar{D}^*$ channel close to threshold, provides $\Gamma = 37^{+26}_{-15} \pm 8$ MeV, which is also compatible with the results of [18] within the large errors. The width of about 50 MeV of [18] for the $X(3922)$ is also in fair agreement with $\Gamma = 29 \pm 10 \pm 2$ MeV of [27].

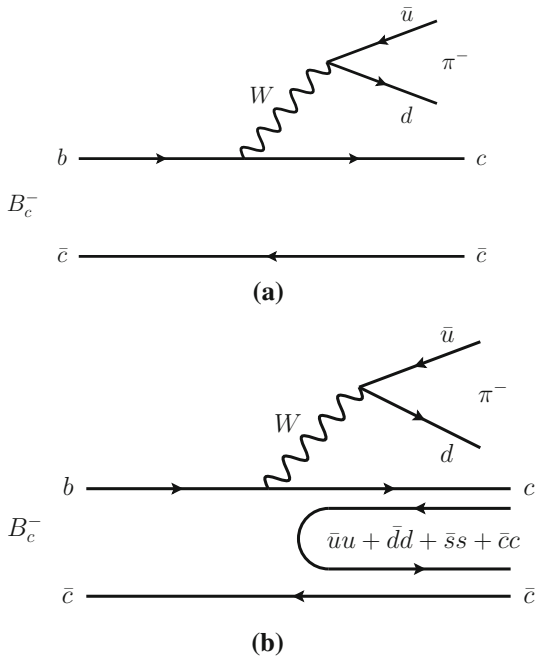

Fig. 1 **a** Microscopic quark picture of $B_c^- \to \pi^- c\bar{c}$ decay. **b** Hadronization through $\bar{q}q$ creation with vacuum quantum numbers

2 Formalism

We look into the B_c^- decay mechanism at quark level depicted in Fig. 1a.

The mechanism qualifies as external emission [28] and is both Cabibbo favored in Wud vertex, and color favored (the Wbc vertex is also the least Cabibbo suppressed of the b decays). Then the final c quark from b decay and the spectator $\bar{c}$ quark from the B_c^- hadronize, with the incorporation of $\bar{q}q$ with the quantum numbers of the vacuum (see Fig. 1b) to give two mesons. The resulting two mesons are easily obtained by writing

$$H = \sum_{i=1}^{4} c\bar{q}_i q_i \bar{c} = \sum_{i=1}^{4} M_{4i}\, M_{i4} = (M^2)_{44},$$

where M_{ij} is the $q\bar{q}$ matrix with the u, d, s, c quarks. However, it is convenient to write the $q\bar{q}$ matrix in terms of physical mesons, in this case vector mesons as

$$M_{ij} \to V = \begin{pmatrix} \frac{1}{\sqrt{2}}\rho^0 + \frac{1}{\sqrt{2}}\omega & \rho^+ & K^{*+} & \bar{D}^{*0} \\ \rho^- & -\frac{1}{\sqrt{2}}\rho^0 + \frac{1}{\sqrt{2}}\omega & K^{*0} & \bar{D}^{*-} \\ K^{*-} & \bar{K}^{*0} & \phi & D_s^{*-} \\ D^{*0} & D^{*+} & D_s^{*+} & J/\psi \end{pmatrix}, \quad (1)$$

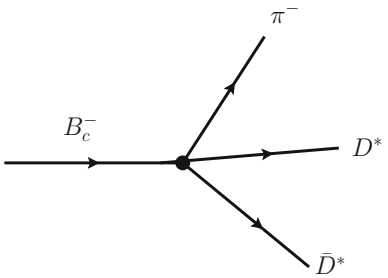

Fig. 2 Tree level contribution corresponding to the hadronization depicted in Fig. 1b

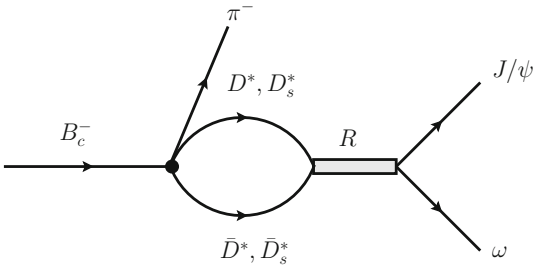

Fig. 3 Mechanism to produce the $J/\psi\omega$ final state through rescattering of the $D^*\bar{D}^*$ and $D_s^*\bar{D}_s^*$ components. R is either the $X(3922)$ (2^{++}) or $X(3943)$ (0^{++})

and we get

$$|H\rangle = D^{*0}\bar{D}^{*0} + D^{*+}\bar{D}^{*-} + D_s^{*+}\bar{D}_s^{*-} + J/\psi J/\psi. \quad (2)$$

The intrinsic phase convention for isospin multiplets in $(D^{*+}, -D^{*0})$, $(\bar{D}^{*0}, D^{*-})$ indicates that the isospin combination of H is $I = 0$, as it should be since it comes from $c\bar{c}$. Thus, we can write

$$|H\rangle = \sqrt{2}|D^*\bar{D}^*\rangle + |D_s^*\bar{D}_s^*\rangle, \quad (3)$$

where we have neglected the $J/\psi J/\psi$ component which is far beyond in energy from our range of concern. In addition, the coupling of the resonances found in [18] to $J/\psi J/\psi$ is negligibly small.

The combination of $|H\rangle$ in Eq. (3) accounts only for the flavor composition. We need to take into account the spin-angular momentum structure of the vertices. If we produce a $0^+[0^{++}]$ $D^*\bar{D}^*$ state we have $0^- \to 0^-\, 0^+$ transition and we adopt the common choice of taking the lowest possible angular momentum in the vertex, $L = 0$. The s-wave and the $J^P = 1^-$ of the D^* leads us to a vertex of the type

$$A'\,\boldsymbol{\epsilon}\cdot\boldsymbol{\epsilon}\,' \quad (4)$$

with $\boldsymbol{\epsilon}$, $\boldsymbol{\epsilon}\,'$ the polarization vertices of D^*, $\bar{D}^*$. Note that we shall work in the rest frame of the resonances produced, where D^*, $\bar{D}^*$ momenta are small with respect to their masses and then we neglect the ϵ^0 component. On the other hand, if we produce a 2^{++} state, the $0^- \to 0^-, 2^+$ requires $L = 2$ and we shall then take the D-wave structure

$$B\left(\boldsymbol{\epsilon}\cdot\mathbf{k}\boldsymbol{\epsilon}\,'\cdot\mathbf{k} - \frac{1}{3}|\mathbf{k}|^2\,\boldsymbol{\epsilon}\cdot\boldsymbol{\epsilon}\,'\right), \quad (5)$$

where $\mathbf{k}$ is the momentum of the pion. Hence, the tree level amplitude for $B_s^- \to \pi^- D^*\bar{D}^*$ shown in Fig. 2 is given by

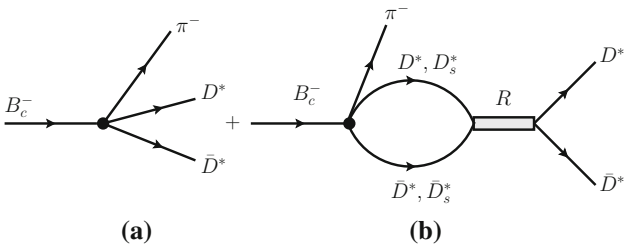

Fig. 4 Mechanism to produce the $D^*\bar{D}^*$ in the final state through tree level (**a**) and rescattering (**b**). R is either the $X(3922)$ (2^{++}) or $X(3943)$ (0^{++})

$$t^{tree}_{B_c\to\pi^- D^*\bar{D}^*} = \sqrt{2}\Big[A\,|\mathbf{k}_{av}|^2\,\boldsymbol{\epsilon}\cdot\boldsymbol{\epsilon}\,' + B\left(\boldsymbol{\epsilon}\cdot\mathbf{k}\,\boldsymbol{\epsilon}\,'\cdot\mathbf{k} - \frac{1}{3}|\mathbf{k}|^2\,\boldsymbol{\epsilon}\cdot\boldsymbol{\epsilon}\,'\right)\Big], \quad (6)$$

where we have substituted A' of Eq. (4) by $A\,|\mathbf{k}_{\rm av}|^2$, with $\mathbf{k}_{\rm av}$, an average value of $\mathbf{k}$, just to make A and B have the same dimension. We take $|\mathbf{k}_{\rm av}| = 1000$ MeV.

After the first step for $D^*\bar{D}^*$ and $D_s^*\bar{D}_s^*$ production, these mesons undergo final state interaction, as depicted in Figs. 3 and 4, to produce $J/\psi\omega$ and $D^*\bar{D}^*$ in the final state. In the case of $J/\psi\omega$ production shown in Fig. 3, since this state is not primarily produced in $|H\rangle$, it is produced through rescattering via the resonances $X(3922)$ and $X(3943)$. In the case of $D^*\bar{D}^*$ production, shown in Fig. 4, it proceeds via tree level (primary production, Fig. 4a) and rescattering (Fig. 4b).

Analytically, we have

$$t_{J/\psi\omega} = A\,|\mathbf{k}_{\rm av}|^2\,\boldsymbol{\epsilon}\cdot\boldsymbol{\epsilon}\,'\,t_1 + B\left(\boldsymbol{\epsilon}\cdot\mathbf{k}\,\boldsymbol{\epsilon}\,'\cdot\mathbf{k} - \frac{1}{3}|\mathbf{k}|^2\,\boldsymbol{\epsilon}\cdot\boldsymbol{\epsilon}\,'\right)\,t_2, \quad (7)$$

where

$$t_1 = \sqrt{2}G_{D^*\bar{D}^*}\left(M_{\rm inv}^{J/\psi\omega}\right)\,t^I_{D^*\bar{D}^*\to J/\psi\omega}\left(M_{\rm inv}^{J/\psi\omega}\right) + G_{D_s^*\bar{D}_s^*}\left(M_{\rm inv}^{J/\psi\omega}\right)\,t^I_{D_s^*\bar{D}_s^*\to J/\psi\omega}\left(M_{\rm inv}^{J/\psi\omega}\right), \quad (8)$$

and

$$t_2 = \sqrt{2} G_{D^*\bar{D}^*}\left(M_{\rm inv}^{J/\psi\omega}\right) t^{II}_{D^*\bar{D}^*\to J/\psi\omega}\left(M_{\rm inv}^{J/\psi\omega}\right) + G_{D_s^*\bar{D}_s^*}\left(M_{\rm inv}^{J/\psi\omega}\right) t^{II}_{D_s^*\bar{D}_s^*\to J/\psi\omega}\left(M_{\rm inv}^{J/\psi\omega}\right), \quad (9)$$

while for $D^*\bar{D}^*$ production we have

$$t_{D^*\bar{D}^*} = A\,|\mathbf{k}_{\rm av}|^2 \boldsymbol{\epsilon}\cdot\boldsymbol{\epsilon}\,' t_3 + B\left(\boldsymbol{\epsilon}\cdot\mathbf{k}\,\boldsymbol{\epsilon}\,'\cdot\mathbf{k} - \frac{1}{3}|\mathbf{k}|^2\boldsymbol{\epsilon}\cdot\boldsymbol{\epsilon}\,'\right) t_4, \quad (10)$$

with

$$t_3 = \sqrt{2} + \sqrt{2} G_{D^*\bar{D}^*}\left(M_{\rm inv}^{D^*\bar{D}^*}\right) t^{I}_{D^*\bar{D}^*\to D^*\bar{D}^*}\left(M_{\rm inv}^{D^*\bar{D}^*}\right) + G_{D_s^*\bar{D}_s^*}\left(M_{\rm inv}^{D^*\bar{D}^*}\right) t^{I}_{D_s^*\bar{D}_s^*\to D^*\bar{D}^*}\left(M_{\rm inv}^{D^*\bar{D}^*}\right), \quad (11)$$

and

$$t_4 = \sqrt{2} + \sqrt{2} G_{D^*\bar{D}^*}\left(M_{\rm inv}^{D^*\bar{D}^*}\right) t^{II}_{D^*\bar{D}^*\to D^*\bar{D}^*}\left(M_{\rm inv}^{D^*\bar{D}^*}\right) + G_{D_s^*\bar{D}_s^*}\left(M_{\rm inv}^{D^*\bar{D}^*}\right) t^{II}_{D_s^*\bar{D}_s^*\to D^*\bar{D}^*}\left(M_{\rm inv}^{D^*\bar{D}^*}\right), \quad (12)$$

where I, II stand for the 0^{++} and 2^{++} states, respectively. Since the $\boldsymbol{\epsilon}\cdot\boldsymbol{\epsilon}\,'$ and $\boldsymbol{\epsilon}\cdot\mathbf{k}\,\boldsymbol{\epsilon}\,'\cdot\mathbf{k} - \frac{1}{3}|\mathbf{k}|^2\boldsymbol{\epsilon}\cdot\boldsymbol{\epsilon}\,'$ structures filter spin 0 and 2 respectively, the structure is kept in the iterations implicit in Eqs. (8), (9), (11) and (12). The G functions in the former equations are the vector loop functions for the intermediate $D^*\bar{D}^*$, $D_s^*\bar{D}_s^*$ in Figs. 3 and 4b. They are regularized in Ref. [18] using dimensional regularization with the subtraction constant $a = -2.07$ and $\mu = 1000$ MeV. Here, we follow the prescription of Refs. [17,29] and we use the cutoff method with $q_{\rm max}$ fixed to reproduce the results of Ref. [18]. In the former equations A and B are functions (we take them as constants in the limited range of invariant mass studied) which have to do with the weight of the weak process and hadronization before the final state interaction is taken into account. We shall vary A and B within a reasonable range to see the results.

With the amplitudes of Eqs. (7) and (10) the mass distributions, summing $|t|^2$ over the final vector polarizations, given by

$$\frac{d\Gamma}{dM_{\rm inv}^{J/\psi\omega}} = \frac{1}{(2\pi)^3}\frac{k'\tilde{p}_\omega}{4M_{B_c}^2}\left(3|A|^2|\mathbf{k}_{\rm av}|^4|t_1|^2 + \frac{2}{3}|B|^2|\mathbf{k}|^4|t_2|^2\right), \quad (13)$$

$$\frac{d\Gamma}{dM_{\rm inv}^{D^*\bar{D}^*}} = \frac{1}{(2\pi)^3}\frac{k'\tilde{p}_{D^*}}{4M_{B_c}^2}\left(3|A|^2|\mathbf{k}_{\rm av}|^4|t_3|^2 + \frac{2}{3}|B|^2|\mathbf{k}|^4|t_4|^2\right), \quad (14)$$

where k' is the π momentum in the B_c^- rest frame, $\tilde{p}_\omega$ the ω momentum in the $J/\psi\omega$ rest frame and k the pion momentum in the $J/\psi\omega$ rest frame for the $J/\psi\omega$ final state,

$$k' = \frac{\lambda^{1/2}(M_{B_c}^2, m_\pi^2, M_{\rm inv}^{2\,J/\psi\omega})}{2M_{B_c}}, \quad (15)$$

$$k = \frac{\lambda^{1/2}(M_{B_c}^2, m_\pi^2, M_{\rm inv}^{2\,J/\psi\omega})}{2M_{\rm inv}^{J/\psi\omega}}, \quad (16)$$

$$\tilde{p}_\omega = \frac{\lambda^{1/2}(M_{\rm inv}^{2\,J/\psi\omega}, M_{J/\psi}^2, m_\omega^2)}{2M_{\rm inv}^{J/\psi\omega}}, \quad (17)$$

with $\lambda(x,y,z) = x^2+y^2+z^2-2xy-2xz-2yz$. For the $D^*\bar{D}^*$ final state in k, k' we change $M_{\rm inv}^{J/\psi\omega}$ to $M_{\rm inv}^{D^*\bar{D}^*}$ and $\tilde{p}_{D^*}$ is like $\tilde{p}_\omega$ changing also $M_{\rm inv}^{J/\psi\omega}$ by $M_{\rm inv}^{D^*\bar{D}^*}$ and $M_{J/\psi}$, m_ω by M_{D^*}, $M_{\bar{D}^*}$.

We get the amplitudes t^I and t^{II} from Ref. [18]. We take them using the Flatté form of the amplitude in terms of the couplings obtained in Ref. [18] and the width. The couplings are given in Table 1.

The amplitudes are given by

$$t^i_{D^*\bar{D}^*,\,j} = \frac{g^{(i)}_{R,\,D^*\bar{D}^*}\, g^{(i)}_{R,\,j}}{M_{\rm inv}^{2\,j} - M_{R_i}^2 + iM_{R_i}\Gamma_{R_i}}, \quad (18)$$

with $i = I,\ II$, and $j = J/\psi\omega$ or $D^*\bar{D}^*$. We also have

$$t^i_{D_s^*\bar{D}_s^*,\,j} = \frac{g^{(i)}_{R,\,D_s^*\bar{D}_s^*}\, g^{(i)}_{R,\,j}}{M_{\rm inv}^{2\,j} - M_{R_i}^2 + iM_{R_i}\Gamma_{R_i}}, \quad (19)$$

where the width is taken as

$$\Gamma_{R_i} = \Gamma_0^{(i)} + \Gamma^{(i)}_{J/\psi\omega} + \Gamma^{(i)}_{D^*\bar{D}^*}, \quad (20)$$

with

$$\Gamma^{(i)}_{J/\psi\omega} = \frac{|g^i_{R,\,J/\psi\omega}|^2}{8\pi M_{R_i}^2}\,\tilde{p}_\omega, \quad (21)$$

and $\tilde{p}_\omega$ given by Eq. (17) as a function of $M_{\rm inv}^{J/\psi\omega}$ or $M_{\rm inv}^{D^*\bar{D}^*}$ depending on the reaction studied, and

$$\Gamma^{(i)}_{D^*\bar{D}^*} = \frac{|g^i_{R,\,D^*\bar{D}^*}|^2}{8\pi M_{R_i}^2}\,\tilde{p}_{D^*}\Theta(M_{\rm inv} - 2M_{D^*}), \quad (22)$$

with $\tilde{p}_{D^*}$ as $\tilde{p}_\omega$ in Eq. (17) with the changes $M_{J/\psi} \to M_{D^*}$, $M_\omega \to M_{\bar{D}^*}$, and $M_{\rm inv} \to M_{\rm inv}^{J/\psi\omega}$ or $M_{\rm inv}^{D^*\bar{D}^*}$ depending on the reaction studied. The width $\Gamma_0^{(i)}$ in Eq. (20) accounts for the channels different of $J/\psi\omega$ and $D^*\bar{D}^*$, mostly the light channels, such that $\Gamma_0^{(i)}$ is practically constant and we take

Table 1 Couplings g_i of the 0^{++} and 2^{++} resonances to the relevant channels, in units of MeV

$D^*\bar{D}^*$	$D_s^*\bar{D}_s^*$	$K^*\bar{K}^*$	$\rho\rho$
$\sqrt{s}_{pole} = 3943 + i7.4$, $I^G[J^{PC}] = 0^+[0^{++}]$			
$18{,}810 - i682$	$8426 + i1933$	$10 - i11$	$-22 + i47$
$\omega\omega$	$\phi\phi$	$J/\psi J/\psi$	
$1348 + i234$	$-1000 - i150$	$417 + i64$	
$\omega J/\psi$	$\phi J/\psi$	$\omega\phi$	
$-1429 - i216$	$889 + i196$	$-215 - i107$	
$\sqrt{s}_{pole} = 3922 + i26$, $I^G[J^{PC}] = 0^+[2^{++}]$			
$21{,}100 - i1802$	$1633 + i6797$	$42 + i14$	$-75 + i37$
$\omega\omega$	$\phi\phi$	$J/\psi J/\psi$	
$1558 + i1821$	$-904 - i1783$	$1783 + i197$	
$\omega J/\psi$	$\phi J/\psi$	$\omega\phi$	
$-2558 - i2289$	$918 + i2921$	$91 - i784$	

$$\Gamma_0^{(i)} = \Gamma_{R_i} - \Gamma^{(i)}_{J/\psi\omega}(M_{\rm inv}^{J/\psi\omega} = M_{R_i}). \tag{23}$$

Note that in Eq. (22), $\Gamma^{(i)}_{D^*\bar{D}^*}$ only starts above the $D^*\bar{D}^*$ threshold, but since the coupling of the resonance to this channel is so large, it grows fast above threshold giving rise to the Flatté effect.

In [18] only the vector-vector channels were used in the coupled channel calculation. The $D^*\bar{D}^*$ channel can also couple to $D\bar{D}$ via pion exchange. This contribution was taken into account in [18], including box diagrams with $D\bar{D}$ in the intermediate states. As shown there, the inclusion of these channels barely changes the mass of the states and modifies the width in only a few MeV. We thus ignore it here. A possible $\eta_c\eta$ decay channel is even more suppressed because if involves the D exchange, rather than the pion, and the heavy mass reduces the strength of the propagator.

3 Results

We will present the invariant mass distribution in arbitrary units, but $\frac{d\Gamma}{dM_{\rm inv}^{J/\psi\omega}}$ and $\frac{d\Gamma}{dM_{\rm inv}^{D^*\bar{D}^*}}$ will have the same normalization. For this purpose, we take $A = 1$ and look at the results for different values of B. Since A and B have been normalized to have the same dimensions, providing similar strength for the two terms for $A = B$, we will take values of B close to 0.5, 1, 1.5 and 2. The values chosen for this ratio are not arbitrary. Using the $^3P_0$ model to implement the $q\bar{q}$ hadronization [30] and Racah algebra one can relate the states for scalar and vector or tensor production. This exercise is done in [31] to relate pseudoscalar and vector production in $\Lambda_b \to \pi^-(D_s^-)\Lambda_c(2595)$, $\pi^-(D_s^-)\Lambda_c(2625)$ decays and the difference results in a factor of $\sqrt{3}$. Furthermore, we have empirical information more closely related to the problem discussed here in the $D^+ \to \pi^+ f_0(1370)$ and $D^+ \to \pi^+ f_2(1270)$. Indeed, the $f_0(1370)$ and $f_2(1270)$ are obtained from the interaction of $\rho\rho$ in [10–12]. They are the equivalent in the light sector to the $X(3940)$ and $X(3930)$ studied here in the heavy quark sector. The branching ratios are $(8 \pm 4) \times 10^{-5}$ and $(4.8 \pm 0.8) \times 10^{-4}$, respectively, with the resonances decaying to $\pi^+\pi^-$ [16]. Correcting by $\frac{3}{2}$ to account for $\pi^0\pi^0$ decay of the $I = 0$ state, and dividing by the branching fractions to $\pi\pi$ from the PDG [16], we obtain the rates $(4.6 \pm 2.3) \times 10^{-4}$ and $(8.5 \pm 1.4) \times 10^{-4}$ for the production of the two resonances irrespectively of their decay mode. As we can see these rates differ by about a factor of two. This also indicates a preference for value of B/A bigger than 1 in our case. We show in Fig. 5 the results of $\frac{d\Gamma}{dM_{\rm inv}^{J/\psi\omega}}$ and in Fig. 6 for $\frac{d\Gamma}{dM_{\rm inv}^{D^*\bar{D}^*}}$ for these different values. The absolute normalization is arbitrary and the shape changes a bit since one gives more strength to one or another resonance changing B.

In Fig. 5 we see that due to the proximity of the two resonances, and the fact that both of them can be produced in this

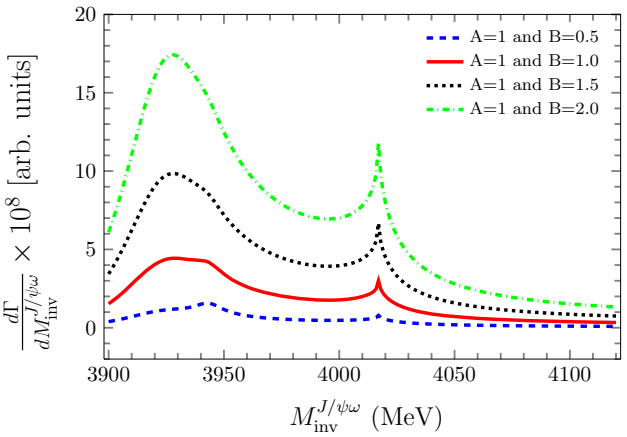

Fig. 5 $\frac{d\Gamma}{dM_{\rm inv}^{J/\psi\omega}}$ results for the different values of the parameter B

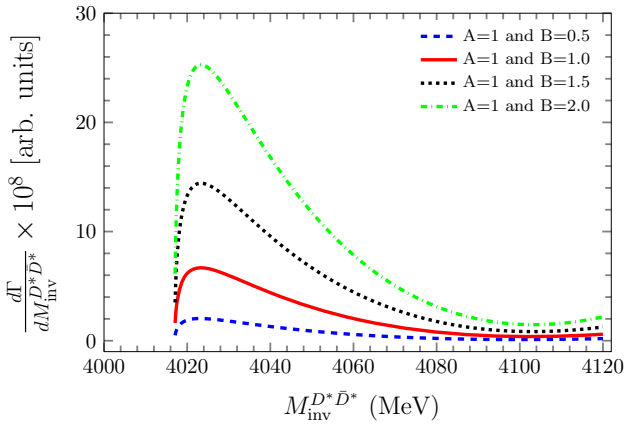

Fig. 6 $\frac{d\Gamma}{dM_{\rm inv}^{D^*\bar{D}^*}}$ results for the different values of the parameter B. The normalization is the same as in Fig. 5

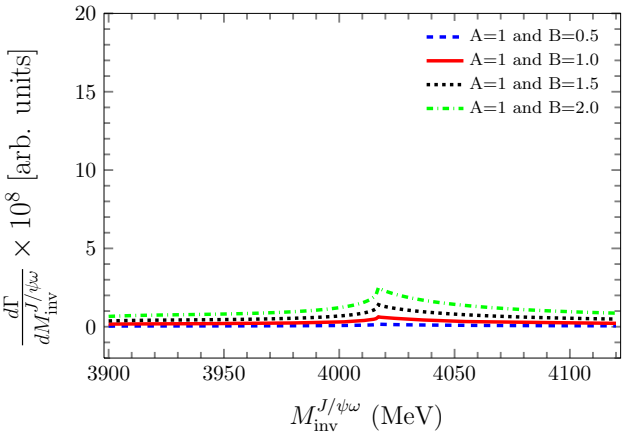

Fig. 7 $\frac{d\Gamma}{dM_{\rm inv}^{J/\psi\omega}}$ results for the different values of the parameter B, but with the mass of the two resonances at 3800 MeV

Table 2 Ratio R between the maximum of the $D^*\bar{D}^*$ mass distribution in Fig. 6 and the strength of the cusp at the $D^*\bar{D}^*$ threshold in Fig. 5

$A = 1.0$			
$B = 0.5$	$B = 1.0$	$B = 1.5$	$B = 2.0$
$R = 2.57$	$R = 2.22$	$R = 2.16$	$R = 2.13$

reaction, the two peaks actually merge into a broader one, although a precise measurement could maybe allow a separation of the two peaks, particularly if a partial wave analysis is done that separates the two different spin resonances. Interesting, however, is the fact that the cusp appears always at the same place, the $D^*\bar{D}^*$ threshold. The other relevant feature is that its strength grows with increasing weight of the tensor resonance, indicating that the cusp is basically tied to the 2^{++} $X(3930)$ state.

In Fig. 6 we show the $D^*\bar{D}^*$ mass distribution in the $B_c^- \to \pi^- D^*\bar{D}^*$ decay. We observe a distribution quite different from ordinary phase space, sticking close to threshold, indicating that it is influenced by a resonance below threshold. Its strength also grows with increasing strength of the tensor resonance, which establishes a link between this state and the $D^*\bar{D}^*$ distribution.

Very interesting is the ratio of the strengths of $\frac{d\Gamma}{dM_{\rm inv}^{J/\psi\omega}}$ at the peak of the cusp of the $D^*\bar{D}^*$ threshold versus the strength at the peak of $\frac{d\Gamma}{dM_{\rm inv}^{D^*\bar{D}^*}}$. We show these numbers in Table 2 for different values of B. As we can see, this ratio is relatively stable and tied to the dynamically generated nature of the two resonances discussed.

The fact that the ratio R is essentially independent on the strength B of the tensor resonance indicates that it is this resonance in practice the one that is responsible for both the cusp in the $J/\psi\omega$ and the $D^*\bar{D}^*$ mass distributions in the $B_c^- \to \pi^- D^*\bar{D}^*$ reaction.

It is interesting to further investigate the role of the resonance in the $D^*\bar{D}^*$ cusp. Certainly, the fact that a cusp in $D^*\bar{D}^*$ appears observing the $J/\psi\omega$ invariant mass indicates that these channels are coupled, otherwise there would be no cusp. Even more, for the particular case, since $J/\psi\omega$ does not appear in the contribution of primary formed states of Eq. (2), the presence of a cusp at the $D^*\bar{D}^*$ threshold implies a transition from $D^*\bar{D}^*$ or $D_s^*\bar{D}_s^*$ to $J/\psi\omega$. This information is already helpful by itself, indicating the presence of coupled channels. On the other hand, we can simulate a situation where we have coupled channels but we have no resonances. Without changing the formalism we can artificially place the positions of the resonances, at 3800 MeV, for instance, and see what happens. We show the results in Fig. 7 and we can see that the resonances do not show up in the range of energies of Fig. 5, which we also consider in Fig. 7. We still see a cusp at the $D^*\bar{D}^*$ threshold, which is a necessary consequence of the coupled channels, with or without resonances. However, for the same strength of B/A, the strength of the cusp is much weaker than in Fig. 5, when we have the presence of the resonances nearby. Also the shape of the cusp is sharper in the presence of the resonances, as seen in Fig. 5.

4 Conclusions

We have looked into the $B_c^- \to J/\psi\omega$ decay and in particular in the $J/\psi\omega$ mass distribution. We find that this observable is much influenced by the role of the $X(3940)$ and $X(3930)$ resonances, which in Ref. [18] appear dynamically generated from the vector-vector meson interaction in the charm sector. These resonances couple mostly to $D^*\bar{D}^*$ in 2^{++} and 0^{++}, respectively. In order to find support for this nature of the resonances we stress two particular features: the first one is to observe that $J/\psi\omega$ is not the main channel for

this resonances, but $D^*\bar{D}^*$. As a consequence, one finds a strong cusp at the $D^*\bar{D}^*$ threshold in the $J/\psi\omega$ mass distribution. The other feature is that since the resonances are tied to $D^*\bar{D}^*$, they should influence the $D^*\bar{D}^*$ mass distribution close to threshold in the $B_c^- \to \pi^- D^*\bar{D}^*$ reaction. What we find is that, within uncertainties tied to our relative ignorance of the weight by which the $X(3940)$ and $X(3930)$ resonances are produced, the ratio of the strength at the cusp peak and the strength at the maximum of the $D^*\bar{D}^*$ mass distribution are related and quite independent of the relative weight of these two resonances. This is because the $D^*\bar{D}^*$ mass distribution is more influenced by the $X(3930)$ resonance that has a larger width.

In addition we observe also a peak around 3930–3940 MeV in the $J/\psi\omega$ mass distribution, corresponding to the excitation of these two resonances, and show that the cusp at the $D^*\bar{D}^*$ threshold has similar strength as the peak. All these features, when observed, should serve to support the molecular nature of these resonances and we can only encourage the performance of the experiments.

Acknowledgements L. R. Dai would like to acknowledge the support from the State Scholarship Fund of China (no. 201708210057) and the National Natural Science Foundation of China (no. 11575076). J. M. Dias thanks the Fundação de Amparo à Pesquisa do Estado de São Paulo (FAPESP) for support by FAPESP Grant 2016/22561-2. This work is partly supported by the Spanish Ministerio de Economia y Competitividad and European FEDER funds under the contract number FIS2011-28853-C02-01, FIS2011-28853-C02-02, FIS2014-57026-REDT, FIS2014-51948-C2-1-P, and FIS2014-51948-C2-2-P, and the Generalitat Valenciana in the program Prometeo II-2014/068 (EO).

References

1. H.X. Chen, W. Chen, X. Liu, S.L. Zhu, Phys. Rep. **639**, 1 (2016)
2. F.K. Guo, C. Hanhart, U.G. Meissner, Q. Wang, Q. Zhao, B.S. Zou, arXiv:1705.00141 [hep-ph]
3. M. Karliner, J.L. Rosner, T. Skwarnicki, arXiv:1711.10626 [hep-ph]
4. L. Roca, E. Oset, Phys. Rev. D **82**, 054013 (2010)
5. J. Yamagata-Sekihara, L. Roca, E. Oset, Phys. Rev. D **82**, 094017 (2010). Erratum: [Phys. Rev. D **85**, 119905 (2012)]
6. C.W. Xiao, M. Bayar, E. Oset, Phys. Rev. D **86**, 094019 (2012)
7. A. Martinez Torres, K.P. Khemchandani, E. Oset, Phys. Rev. C **79**, 065207 (2009)
8. D. Jido, Y. Kanada-En'yo, Phys. Rev. C **78**, 035203 (2008)
9. E. Oset et al., Acta Phys. Polon. B **47**, 357 (2016)
10. R. Molina, D. Nicmorus, E. Oset, Phys. Rev. D **78**, 114018 (2008)
11. L.S. Geng, E. Oset, Phys. Rev. D **79**, 074009 (2009)
12. L.S. Geng, R. Molina, E. Oset, Chin. Phys. C **41**(12), 124101 (2017)
13. E. Oset et al., Int. J. Mod. Phys. E **25**, 1630001 (2016)
14. R. Aaij et al. [LHCb Collaboration], Phys. Rev. D **95**(1), 012002 (2017)
15. R. Aaij et al. [LHCb Collaboration], Phys. Rev. Lett. **118**(2), 022003 (2017)
16. C. Patrignani et al. [Particle Data Group], Chin. Phys. C **40**(10), 100001 (2016)
17. E. Wang, J.J. Xie, L.S. Geng, E. Oset, arXiv:1710.02061 [hep-ph]
18. R. Molina, E. Oset, Phys. Rev. D **80**, 114013 (2009)
19. X. Liu, S.L. Zhu, Phys. Rev. D **80**, 017502 (2009). Erratum: [Phys. Rev. D **85**, 019902 (2012)]
20. T. Branz, T. Gutsche, V.E. Lyubovitskij, Phys. Rev. D **80**, 054019 (2009)
21. X. Chen, X.LR. Shi, X. Guo, arXiv:1512.06483 [hep-ph]
22. M. Karliner, J.L. Rosner, Nucl. Phys. A **954**, 365 (2016)
23. M. Ablikim et al. [BESIII Collaboration], arXiv:1712.09240 [hep-ex]
24. K. Abe et al. [Belle Collaboration], Phys. Rev. Lett. **94**, 182002 (2005)
25. K. Abe et al. [Belle Collaboration], Phys. Rev. Lett. **98**, 082001 (2007)
26. P. Pakhlov et al. [Belle Collaboration], Phys. Rev. Lett. **100**, 202001 (2008)
27. S. Uehara et al. [Belle Collaboration], Phys. Rev. Lett. **96**, 082003 (2006)
28. L.L. Chau, Phys. Rep. **95**, 1 (1983)
29. J.J. Wu, B.S. Zou, Phys. Lett. B **709**, 70 (2012)
30. A. Le Yaouanc, L. Oliver, O. Pne, J.-C. Raynal, Phys. Rev. D **8**, 2223 (1973)
31. W.H. Liang, M. Bayar, E. Oset, Eur. Phys. J. C **77**, 39 (2017)